Microbiology (2014), **160**, 1832–1844 **DOI** 10.1099/mic.0.079699-0

Sulfate assimilation pathway intermediate phosphoadenosine 5′-phosphosulfate acts as a signal molecule affecting production of curli fibres in *Escherichia coli*

Elio Rossi,[1] Sara Motta,[2] Pierluigi Mauri[2] and Paolo Landini[1]

[1]Department of Biosciences, Università degli Studi di Milano, Via Celoria, 26, 20133 Milan, Italy

[2]Institute of Biomedical Technologies, National Research Council, Via Fratelli Cervi 93, 20090 Segrate, Milan, Italy

Correspondence
Paolo Landini
paolo.landini@unimi.it

Received 3 April 2014
Accepted 11 June 2014

The enterobacterium *Escherichia coli* can utilize a variety of molecules as sulfur sources, including cysteine, sulfate, thiosulfate and organosulfonates. An intermediate of the sulfate assimilation pathway, adenosine 5′-phosphosulfate (APS), also acts as a signal molecule regulating the utilization of different sulfur sources. In this work, we show that inactivation of the *cysH* gene, leading to accumulation of phosphoadenosine 5′-phosphosulfate (PAPS), also an intermediate of the sulfate assimilation pathway, results in increased surface adhesion and cell aggregation by activating the expression of the curli-encoding *csgBAC* operon. In contrast, curli production was unaffected by the inactivation of any other gene belonging to the sulfate assimilation pathway. Overexpression of the *cysH* gene downregulated *csgBAC* transcription, further suggesting a link between intracellular PAPS levels and curli gene expression. In addition to curli components, the Flu, OmpX and Slp proteins were also found in increased amounts in the outer membrane compartment of the *cysH* mutant; deletion of the corresponding genes suggested that these proteins also contribute to surface adhesion and cell surface properties in this strain. Our results indicate that, similar to APS, PAPS also acts as a signal molecule, albeit with a distinct mechanism and role: whilst APS regulates organosulfonate utilization, PAPS would couple availability of sulfur sources to remodulation of the cell surface, as part of a more global effect on cell physiology.

INTRODUCTION

In natural environments, bacteria are exposed to sudden and drastic changes that can trigger specific responses (e.g. induction by a given nutrient of the genes involved in its utilization), but also induce more general effects on cell physiology responses, often involving regulation of motility and/or of cell adhesion factors (Mikkelsen *et al.*, 2011). For instance, availability of *N*-acetylglucosamine induces expression of the *nagBACD* operon and of the *nagE* gene, responsible for its uptake and degradation (Plumbridge, 1991), but it also modulates production of type 1 pili (Sohanpal *et al.*, 2004) and of curli fibres (Barnhart *et al.*, 2006).

In the repertoire of *Escherichia coli* adhesion factors, curli fibres (also known as thin aggregative fimbriae in *Salmonella*) represent a strong determinant for cell aggregation and surface adhesion (Prigent-Combaret *et al.*, 2000). Regulation of curli-encoding genes is extraordinarily complex and responds to a combination of environmental cues, such as low growth temperature ($\leqslant 30$ °C), low osmolarity, slow growth and oxygen availability (Römling *et al.*, 1998a; Gerstel & Römling, 2001, 2003; Tagliabue *et al.*, 2010a). The signal molecules cAMP (Zheng *et al.*, 2004) and c-di-GMP (Kader *et al.*, 2006; Weber *et al.*, 2006), as well as intracellular concentration of pyrimidine nucleotides (Garavaglia *et al.*, 2012), also have a strong impact on curli gene expression. These environmental and physiological signals are relayed by a number of regulatory proteins, including RpoS, OmpR, IHF, H-NS, CpxR, Crl, CRP, MlrA and the MqsR/MqsA toxin/antitoxin system, which affect curli gene transcription either directly or indirectly (Bougdour *et al.*, 2004; Brown *et al.*, 2001; Gerstel *et al.*, 2004; Hung *et al.*, 2001; Prigent-Combaret *et al.*, 2001; Römling *et al.*, 1998a; Soo & Wood, 2013). In addition, at least five non-coding RNAs have been

Abbreviations: APS, adenosine 5′-phosphosulfate; EPS, extracellular polysaccharide; MudPIT, multidimensional protein identification technology; PAP, adenosine 3′,5′-bisphosphate; PAPS, phosphoadenosine 5′-phosphosulfate; q, quantitative; RT, real-time.

One supplementary table and two supplementary figures are available with the online version of this paper.

 079699 © 2014 The Authors *Printed in Great Britain*

shown to take part in post-transcriptional regulation of the curli-related operon *csgDEFG* (Mika & Hengge, 2013). Thus, curli fibre production appears to be a major target for environmental signals promoting cell adhesion.

Sulfur is an essential element and is typically provided in bacterial growth media at millimolar concentrations (Neidhardt *et al.*, 1974). In addition to being a component of the amino acids cysteine and methionine, sulfur is present in reducing compounds (e.g. hydrogen sulfide and glutathione) that play an important role in maintaining the redox conditions of the bacterial cytoplasm and in detoxification of reactive oxygen species (Toledano *et al.*, 2007). *E. coli* can utilize a wide range of sulfur sources, both inorganic (e.g. sulfate, sulfite, thiosulfate) and organic (e.g. cysteine, methionine, organosulfonates), with cysteine being the preferred substrate (van der Ploeg *et al.*, 2001). However, due to its abundance in nature, sulfate is thought to be the main source of sulfur for *E. coli* in most environments. Once taken up by the bacterium, sulfate is readily reduced to hydrogen sulfide by the sulfate assimilation pathway, whose first steps involve activation of sulfate through the formation of two modified nucleotides: adenosine 5′-phosphosulfate (APS) and phosphoadenosine 5′-phosphosulfate (PAPS) (Liu *et al.*, 1994) (Fig. 1). Preferential order in sulfur source utilization is achieved through the activity of two regulatory proteins: CysB, which activates the sulfate assimilation pathway in the absence of exogenous cysteine (Kredich, 1992), and Cbl, whose activation of the organosulfonate utilization genes is counteracted by APS (Bykowski *et al.*, 2002). Such a finely tuned regulatory circuitry determines a clear hierarchy in utilization of sulfur sources: cysteine>sulfate>organosulfonates.

In this study, we provide evidence that inactivation of the *cysH* gene, encoding PAPS reductase, induces overproduction of curli fibres and of other outer membrane proteins, reshaping cell-surface-associated structures. We propose that the effects of the *cysH* mutation are mediated by intracellular PAPS accumulation; thus, PAPS would act as a signal molecule allowing *E. coli* to sense changes in the availability of different sulfur sources and to adapt its physiology accordingly.

METHODS

Bacterial strains and growth conditions. Bacterial strains used in this work are listed in Table 1. For strain construction and manipulation, bacteria were grown in LB medium (10 g tryptone l^{-1}, 5 g yeast extract l^{-1}, 5 g NaCl l^{-1}). If required, antibiotics were added at the following concentrations: ampicillin, 100 μg ml^{-1}; chloramphenicol, 50 μg ml^{-1}; kanamycin, 50 μg ml^{-1}; tetracycline, 25 μg ml^{-1}.

For Congo red- and calcofluor-binding assays, overnight cultures were spotted, using a replicator, on either Congo red- or calcofluor-supplemented agar media. Both media were modifications of the yeast extract-Casamino acid (YESCA) medium (Pratt & Silhavy, 1998), and were composed of 1 % Casamino acids, 0.15 % yeast extract, 0.005 % $MgSO_4$, 0.0005 % $MnCl_2$, 2 % agar to which either 0.004 % Congo red and 0.002 % Coomassie blue (for Congo red medium) or 0.005 % calcofluor (for calcofluor medium) were added after autoclaving. Bacteria were grown for either 24 h at 30 °C or 18 h at 37 °C; phenotypes were better detectable after a further 24–48 h incubation at 4 °C.

For gene expression regulation studies, bacteria were grown in YESCA liquid medium composed of 1 % Casamino acids, 0.15 % yeast extract, 0.005 % $MgSO_4$, 0.0005 % $MnCl_2$. Surface adhesion to polystyrene microtitre plates was analysed on bacterial cultures grown overnight in YESCA at 30 and 37 °C, and adhesion units were determined as described previously (Dorel *et al.*, 1999).

To verify cysteine auxotrophy, bacteria were grown for 24–48 h at 37 °C in either M9 (Carzaniga *et al.*, 2012) or sulfate-free M9 (SF-M9) media with or without supplementation with 0.25 mM cysteine. SF-M9 was obtained substituting $MgSO_4$ with $MgCl_2$ at a final concentration of 1 mM. Glucose (0.4 %) was added as sole carbon source to obtain M9/Glu or SF-M9/Glu media. Growth media were inoculated (1 : 500) with bacteria from overnight cultures in LB medium, after centrifugation and resuspension in PBS to OD_{600} 1.0

Plasmid construction. Plasmids and primers used in this work are listed in Tables 1 and S1 (available in the online Supplementary Material), respectively. For expression of WT CysH protein, the corresponding gene was amplified by PCR from the *E. coli* MG1655 chromosome using primers *cysH_NdeI_for* and *cysH_PstI_rev*, and the resulting product was cloned into pT7-7 vector using the *Nde*I/*Pst*I restriction sites. The pT7*cysH*$_{mut}$ plasmid, carrying a mutant *cysH* allele encoding a protein with a non-functional redox-active centre (Berendt *et al.*, 1995), was constructed by amplifying the *cysH* gene using primers *cysH_NdeI_for* and *cysH_mut_PstI_rev*, resulting in the following substitutions: T→G at nt 715, G→C at nt 716, C→G at nt 724, A→C at nt 725. The four mutations resulted in substitution of both Cys240 and His243 to alanine residues (E**C**GL**H**→E**A**GL**A**). The obtained PCR product was cloned into the pT7-7 vector as the WT allele using the *Nde*I/*Pst*I restriction sites. Both the WT and mutant alleles of the *cysH* gene were verified by sequencing.

Mutant construction. Transposon insertion mutagenesis was carried out using the EZ-Tn5 <R6Kγ*ori*/KAN-2> Transposome kit (Epicentre). Transposon mutagenesis and determination of transposon insertion site by rescue cloning were carried out according to the manufacturer's instructions. *E. coli* MG1655 mutant derivatives were constructed using the λ Red technique (Datsenko & Wanner, 2000). Primers used for gene inactivation and for confirmation of target gene disruption by PCR are listed in Table S1.

Gene expression assays. Gene expression levels were measured through quantitative real-time (qRT)-PCR as described previously (Gualdi *et al.*, 2007) using 16S RNA as reference gene. RNA was extracted from overnight cultures grown in YESCA medium at 30 or 37 °C in full aeration, achieved by constant shaking at 100 r.p.m. The complete list of primers used for amplification is reported in Table S1.

Analysis of the outer membrane compartment. For proteomic analysis, outer membrane-protein-enriched samples were obtained using the *N*-lauroylsarcosinate method as described previously (Gualdi *et al.*, 2007). Enriched samples were treated with RapiGest SF (Waters) and digested with trypsin as described previously (Comunian *et al.*, 2011). Digested samples were then analysed by 2D micro-liquid chromatography coupled to ion-trap MS (2DC-MS/MS) using the ProteomeX-2 configuration (Thermo Electron), as described previously (Palma *et al.*, 2010). The experimental mass spectra produced

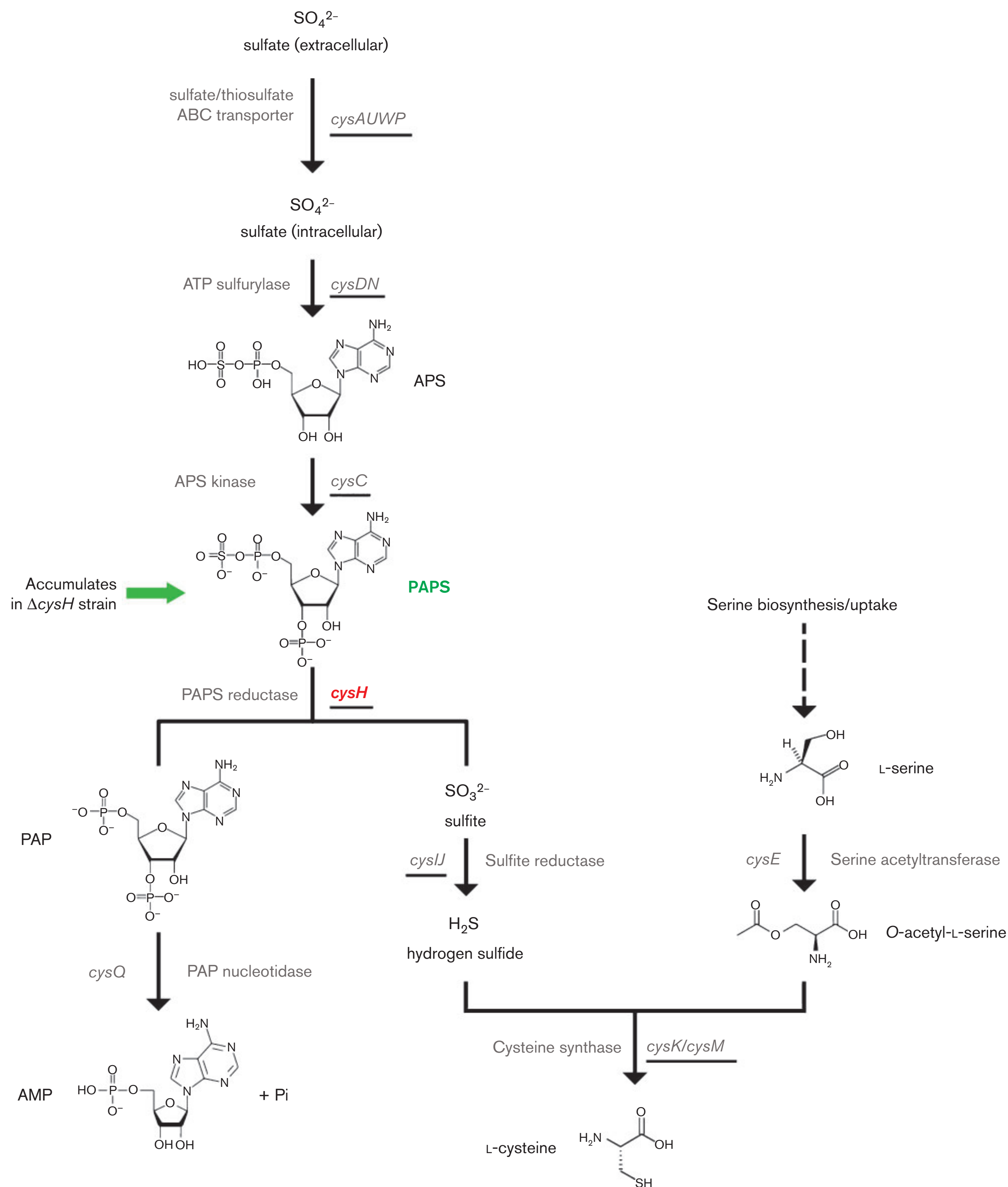

Fig. 1. Sulfate reduction and cysteine biosynthesis pathways in *E. coli* (adapted from http://ecocyc.org). The modified nucleotide PAPS accumulating in the MG1655Δ*cysH* mutant is highlighted in green. The *cysH* gene is highlighted in red. Underlined genes belong to the CysB regulon (Kredich, 1992). More details are provided in the text. PAP, adenosine 3′,5′-bisphosphate.

Table 1. *Escherichia coli* strains and plasmids used in this work

Strain or plasmid	Relevant genotype	Source or reference
Strains		
MG1655	K-12, F^- λ^- *ilvG*$^-$ *rfb-50 rph*-1	Blattner *et al.* (1997)
EB1.3	MG1655 *rpoS*::*tet*	Prigent-Combaret *et al.* (2001)
AM70	MG1655Δ*csgA*::*cat*	Tagliabue *et al.* (2010b)
AM75	MG1655Δ*csgD*::*cat*	Tagliabue *et al.* (2010a)
MG1655*cysH*::Tn*5Kan*	Tn*5*::*kan* transposon inserted at nt 472 of the *cysH* gene coding sequence	This work
MG1655Δ*cysH*	Replacement of the *cysH* gene with a chloramphenicol resistance cassette	This work
MG1655Δ*cysB*	Replacement of the *cysB* gene with a chloramphenicol resistance cassette	This work
MG1655Δ*cysU*	Replacement of the *cysU* gene with a chloramphenicol resistance cassette	This work
MG1655Δ*cysD*	Replacement of the *cysD* gene with a chloramphenicol resistance cassette	This work
MG1655Δ*cysC*	Replacement of the *cysC* gene with a chloramphenicol resistance cassette	This work
MG1655Δ*cysI*	Replacement of the *cysI* gene with a chloramphenicol resistance cassette	This work
MG1655Δ*cysQ*	Replacement of the *cysQ* gene with a kanamycin resistance cassette	This work
MG1655Δ*ompX*	Replacement of the *ompX* gene with a kanamycin resistance cassette	This work
MG1655Δ*slp*	Replacement of the *slp* gene with a kanamycin resistance cassette	This work
MG1655Δ*flu*	Replacement of the *ompX* gene with a tetracycline resistance cassette	This work
MG1655Δ*cysH*Δ*csgA*	Obtained by bacteriophage P1 transduction from AM70 to MG1655*cysH*::Tn*5Kan*	This work
MG1655Δ*cysH*Δ*rpoS*	Obtained by bacteriophage P1 transduction from MG1655Δ*cysH* to EB1.3	This work
MG1655Δ*cysH*Δ*csgD*	Obtained by bacteriophage P1 transduction from MG1655*cysH*::Tn*5Kan* to AM75	This work
MG1655Δ*cysH*Δ*cbl*	Obtained by replacing the *cbl* gene with a kanamycin resistance cassette in MG1655Δ*cysH*	This work
MG1655Δ*cysH*Δ*ompX*	Obtained by replacing the *ompX* gene with a kanamycin resistance cassette in MG1655Δ*cysH*	This work
MG1655Δ*cysH*Δ*slp*	Obtained by replacing the *slp* gene with a kanamycin resistance cassette in MG1655Δ*cysH*	This work
MG1655Δ*cysH*Δ*flu*	Obtained by replacing the *flu* gene with a tetracycline resistance cassette in MG1655Δ*cysH*	This work
Plasmids		
pT7-7	Ampicillin resistance, T7 RNA polymerase-dependent promoter	Gualdi *et al.* (2007)
pT7$cysH_{wt}$	*cysH* gene cloned into pT7-7 vector as a 735 bp *Nde*I/*Pst*I fragment	This work
pT7$cysH_{mut}$	*cysH* allele carrying the mutation resulting in the ECGLH→EAGLA change in the CysH redox site	This work

by MudPIT (multidimensional protein identification technology) analyses were correlated with tryptic peptide sequences by comparison with theoretical mass spectra obtained by *in silico* digestion of the *E. coli* K-12 MG1655 protein database. Outputs were treated with an in-house software called MAProMa (multidimensional algorithm protein map) (Mauri & Dehò, 2008) to identify differentially expressed proteins. Different protein expression was estimated by means of the DAve (differential average) algorithm of MAProMa (Mauri *et al.*, 2005). A DAve value of either >0.1 or <–0.1 is an indication of different relative expression levels between two samples, whilst a DAve value of either 200 or –200 indicates the exclusive presence of a protein in one sample.

Extracellular polysaccharide (EPS) determination was carried out by total sugar quantification using the phenol/H_2SO_4 method as described previously (DuBois *et al.*, 1956).

Statistical analysis. If not otherwise stated, all experiments were performed at least in triplicate and the data were analysed by one-way ANOVA, with a *P* value of 0.05 being significant, using the statistical software package R (R Development Core Team, 2013).

RESULTS

Inactivation of the *cysH* gene affects the production of extracellular structures

Congo red and calcofluor dyes provide an easy way to identify the production of both proteinaceous and EPS surface-exposed structures: Congo red binds with high affinity to amyloid fibres, such as curli fibres (Hammar *et al.*, 1995), and with lower affinity to cellulose (Teather & Wood, 1982) and poly-*N*-acetylglucosamine (Romeo, 1998; Carzaniga *et al.*, 2012); calcofluor binds to various EPS components, in particular cellulose and chitin, resulting in fluorescence detectable by UV light (Harrington & Raper, 1968). In order to identify novel genes involved in the production and regulation of extracellular structures, we performed transposon mutagenesis in the *E. coli* K-12 strain MG1655: mutants were then screened for their phenotype on Congo red and calcofluor medium at both 30 °C, a

temperature permissive for curli production, and 37 °C, a temperature at which production of curli fibres does not take place under standard growth conditions (Römling *et al.*, 1998a). Out of several mutants showing altered phenotypes on both media, one mutant displaying a dark-red phenotype at 30 °C, a red coloration at 37 °C on Congo red and increased fluorescence on calcofluor, was further characterized. Mapping of the EZ-Tn5 <R6Kγ*ori*/KAN-2> transposon indicated that the insertion site lay at nt 472 of the 735 nt *cysH* gene, encoding PAPS reductase. The location of the transposon insertion site suggested inactivation of the *cysH* gene. To verify this hypothesis, we constructed a *cysH* mutant in which the complete coding sequence of the gene was deleted (MG1655Δ*cysH*). As expected, the MG1655Δ*cysH* mutant displayed the same phenotypes as the MG1655*cysH*::Tn*5-kan* strain, i.e. red and fluorescent on Congo red and calcofluor media, respectively (Fig. 2a), and was therefore used in further experiments.

PAPS reductase catalyses the conversion of PAPS into adenosine 3′,5′-bisphosphate (PAP) and sulfite, in the sulfate reduction pathway leading to sulfur assimilation and cysteine biosynthesis (Fig. 1). Indeed, both transposon insertion and *cysH* deletion led, as expected, to cysteine auxotrophy, as shown by the inability of either *cysH* mutant to grow in M9/Glu minimal medium with sulfate as the sole sulfur source (Table 2, Fig. S1). Addition of 0.25 mM cysteine to M9/Glu fully overcame the growth defect (Table 2). The effects of *cysH* inactivation on cell-surface-associated structures could thus be ascribed to cysteine depletion. Indeed, starvation for various nutrients represents an important cue for the induction of the biosynthesis of extracellular structures involved in cellular aggregation and biofilm formation (Gerstel & Römling, 2001). However, MG1655Δ*cysH* showed the same growth rate as its parental strain in liquid YESCA (Fig. S1), which, like the Congo red and calcofluor solid media, contains cysteine from the added Casamino acids and yeast extract, suggesting that the *cysH* mutant was not subjected to cysteine starvation under the conditions used for our phenotypic assays.

To further investigate whether the phenotypic effects due to the *cysH* inactivation could be dependent on either cysteine starvation or accumulation of PAPS, or of any other intermediate in the sulfate assimilation pathway, we constructed deletion mutants in the *cysU*, *cysD*, *cysC* and *cysI* genes, involved in each step of sulfate reduction to hydrogen sulfide (Fig. 1), and in the *cysB* gene, which encodes a positive regulator of the genes belonging to the sulfate assimilation and cysteine biosynthesis pathways (Kredich, 1992). As expected, all mutants were auxotrophic for cysteine (Table 2); however, they displayed WT phenotypes on Congo red and calcofluor plates, with the partial exception of the *cysQ* mutant, showing some fluorescence on calcofluor medium (Fig. 2a). The behaviour of the mutants in the sulfate assimilation pathway confirmed that the phenotypes observed in *cysH* mutant strains were not due to cysteine starvation, but depended on the loss of a functional CysH protein. It could thus be hypothesized that lack of PAPS reductase activity by CysH would cause intracellular PAPS accumulation that, in turn, might result in the Congo red and calcofluor phenotypes of the MG1655Δ*cysH* strain. To further confirm this hypothesis, we complemented a *cysH* mutant with plasmids

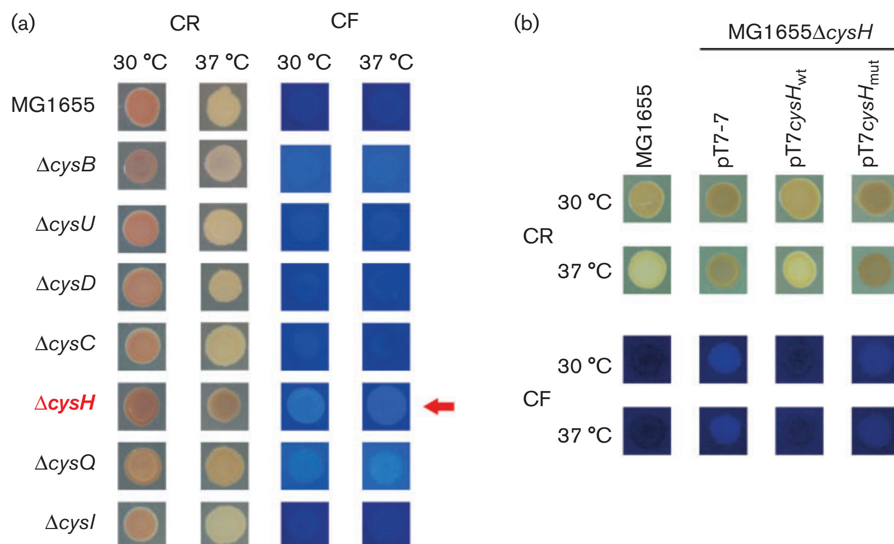

Fig. 2. (a) Congo red (CR) and calcofluor (CF) binding by *E. coli* strains deficient in the sulfate reduction pathway. MG1655 and isogenic mutants in the *cysB*, *cysU*, *cysD*, *cysC*, *cysH* and *cysI* genes were spotted on both media and grown at either 30 (for 24 h) or 37 °C (for 18 h). Plates were incubated at 4 °C for at least 48 h to enhance dye binding. (b) Complementation of MG1655Δ*cysH* with plasmids carrying WT (pT7*cysH*$_{wt}$) and mutant (pT7*cysH*$_{mut}$) alleles of the *cysH* gene. pT7-7, vector.

Table 2. Growth of mutants in genes belonging to the sulfate assimilation pathway in minimal medium with or without cysteine supplementation

Growth was measured as OD_{600} on stationary-phase cultures grown for 24 h at 37 °C with vigorous shaking (>100 r.p.m.) in either M9/Glu or sulfate-free M9/Glu (SF-M9/Glu) media in the presence or absence of 0.25 mM cysteine. Values are the means of three separate experiments with very similar results.

Strain	Growth (OD_{600})			
	M9/Glu		SF-M9/Glu	
	No additions	Cys	No additions	Cys
MG1655	1.43	1.27	0.08	1.02
MG1655*cysH*::Tn5-*kan*	0.01	1.32	NT	NT
MG1655Δ*cysB*	0.02	1.17	0.05	1.02
MG1655Δ*cysU*	0.02	1.27	0.02	0.88
MG1655Δ*cysD*	0.02	1.20	0.03	1.00
MG1655Δ*cysC*	0.01	1.25	0.03	1.01
MG1655Δ*cysH*	0.02	1.33	0.03	1.11
MG1655Δ*cysI*	0.01	1.53	0.03	1.06
MG1655Δ*cysH*/pT7-7	0.02	NT	NT	NT
MG1655Δ*cysH*/pT7$cysH_{wt}$	1.62	NT	NT	NT
MG1655Δ*cysH*/pT7$cysH_{mut}$	0.02	NT	NT	NT

NT, not tested.

carrying either a WT *cysH* gene or a mutant allele, in which two codons encoding C-terminal amino acids identified as the redox-active centre of the enzyme (Berendt *et al.*, 1995) had been substituted to obtain two alanine residues (pT7$cysH_{wt}$ and pT7$cysH_{mut}$, respectively). Production of both the WT and mutated CysH proteins from the pT7-7 plasmid derivatives was clearly detectable on SDS-PAGE (Fig. S2); indeed, although the pT7-7 vector relied on T7 bacteriophage RNA polymerase for gene overexpression, background expression levels were fairly high, probably due to the presence of promoter-like sequences recognized by *E. coli* RNA polymerase (Brombacher *et al.*, 2006). As expected, the mutated CysH protein was not able to rescue MG1655Δ*cysH* auxotrophy for cysteine (Table 2), demonstrating its inability to carry out PAPS reductase activity. Likewise, only the WT *cysH* allele was able to restore WT phenotypes on Congo red and calcofluor medium (Fig. 2b), suggesting strongly that loss of PAPS reductase activity by the CysH protein, leading to intracellular PAPS accumulation, was indeed responsible for cell surface structure alteration in MG1655Δ*cysH*. We attempted to quantify intracellular PAPS concentrations in both the MG1655 strain and its *cysH* mutant derivative using HPLC and MS; unfortunately, neither technique was able to provide a precise PAPS estimation due to the difficulty in distinguishing PAPS from other adenylic nucleotides (data not shown).

Effects of the *cysH* mutation on cell-surface-associated structures

The red phenotype on Congo red medium shown by the MG1655Δ*cysH* mutant was suggestive of increased curli production, whilst calcofluor fluorescence, although usually linked with EPS synthesis, could also depend on curli overproduction, via direct calcofluor binding either to curli fibres or to some curli-associated factor (Uhlich *et al.*, 2014). Indeed, determination of cell-surface-associated polysaccharides did not show any significant differences in EPS amounts between MG1655 and its *cysH* derivative (data not shown), thus suggesting that, in this strain, calcofluor fluorescence was not dependent on EPS. As curli production strongly enhances cell aggregation and adhesion to solid surfaces (Vidal *et al.*, 1998; Cookson *et al.*, 2002), we tested the MG1655Δ*cysH* mutant for its ability to adhere to an abiotic surface. Microtitre adhesion assay revealed a moderate (around twofold), but highly reproducible increase in biofilm formation by the MG1655Δ*cysH* strain at 30 °C (Fig. 3b), whilst no significant differences between strains were observed at 37 °C (data not shown). Phase-contrast microscopy observations provided further confirmation that *cysH* inactivation stimulated the production of aggregative structures, which, again, were more common in cultures grown at 30 than at 37 °C (Fig. 3c). As curli fibres are not produced in *E. coli* K-12 strains at 37 °C, these results were consistent with stimulation of curli production by inactivation of the *cysH* gene. Indeed, an MG1655Δ*cysH*Δ*csgA* double mutant, unable to produce curli, was impaired in both surface adhesion and cell aggregation (Fig. 3b; data not shown). However, the MG1655Δ*cysH*Δ*csgA* mutant still displayed a red phenotype on Congo red and fluorescence on calcofluor medium at both 30 and at 37 °C (Fig. 3a), and a slight increase in surface adhesion when compared with an MG1655Δ*csgA* strain (Fig. 3b). This result suggested that *cysH* inactivation

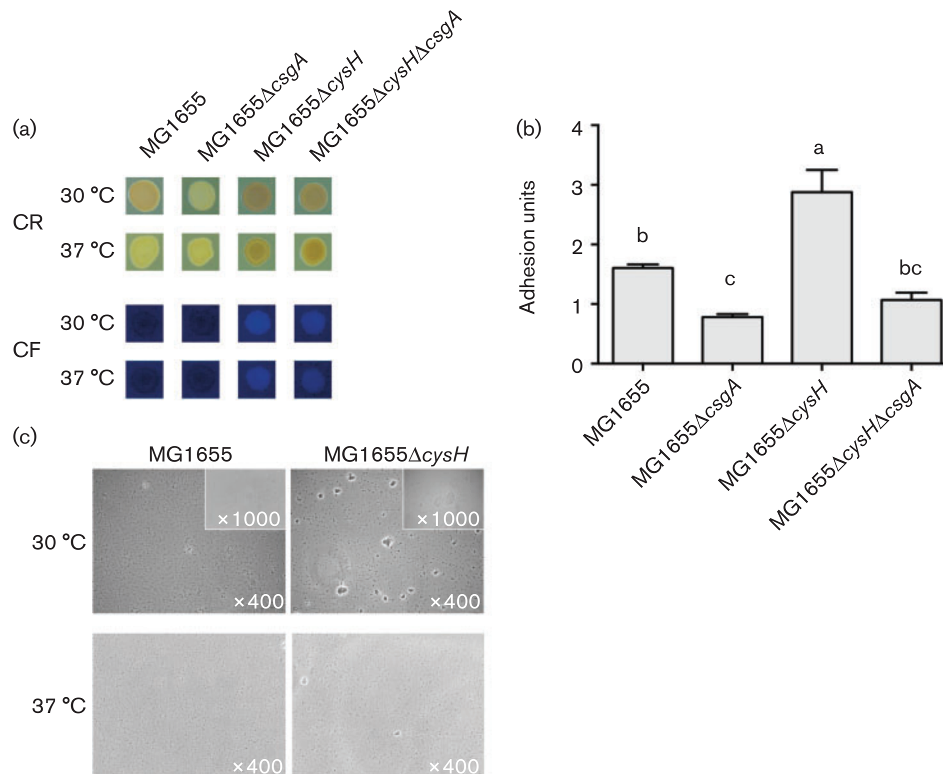

Fig. 3. (a) Phenotypes on Congo red (CR) and calcofluor (CF) media of MG1655 (WT), MG1655Δ*csgA*, MG1655Δ*cysH* and MG1655Δ*cysH*Δ*csgA* strains. Strains were grown at either 30 (for 24 h) or 37 °C (for 18 h). Plates were incubated for 48 h at 4 °C to enhance Congo red and calcofluor binding. (b) Surface adhesion of the same set of strains to polystyrene microtitre plates. The adhesion unit values, assessed as described previously (Dorel *et al.*, 1999), are the mean ± SE of at least four independent experiments. Letters provide the representation for *post hoc* comparisons. According to *post hoc* analysis (Tukey's honest significant difference, $P<0.05$), bars sharing the same letter are not significantly different from each other. (c) Phase-contrast micrographs (main picture, ×400 magnification; inset, ×1000 magnification) of MG1655 and MG1655Δ*cysH* strains grown 16 h in YESCA medium at either 30 or 37 °C. The images were acquired with a digital CCD Leica DFC camera.

promoted the production of an additional factor, able to bind Congo red and calcofluor at both temperatures, and to act as a weak cell aggregation factor.

In order to identify extracellular factors other than curli whose production could be influenced by *cysH* inactivation, we performed protein expression analysis by using MudPIT on an outer membrane-protein-enriched fraction. As the Δ*cysH*-dependent phenotype was observed at both 30 and 37 °C, we focused on proteins showing differential regulation at both temperatures; only a relatively small protein set fulfilled these criteria (Table 3). Protein analysis experiments showed clearly that curli production was increased as a result of *cysH* inactivation; indeed, the main curli subunit CsgA, as well as the CsgF and CsgG proteins, involved in curli assembly and secretion, were present at higher levels in the MG1655Δ*cysH* strain. Although enhanced production of curli proteins occurred at both 30 and 37 °C, Csg proteins were detected at lower levels at 37 than at 30 °C even in MG1655Δ*cysH* (Table 3), in agreement with microscopy observations and surface adhesion experiments (Fig. 3c and data not shown), suggesting that the *cysH* mutation could not fully override temperature-dependence of curli expression.

In addition to curli-related proteins, three more proteins were produced at higher levels in MG1655Δ*cysH*: Slp, a lipoprotein induced under carbon starvation or during the stationary phase (Alexander & St John, 1994), OmpX, an outer membrane protein with unknown function, but related to virulence and to EPS production (Mecsas *et al.*, 1995; Vogt & Schulz, 1999; Otto & Hermansson, 2004), and Flu, also known as Antigen 43, which can mediate cell–cell aggregation and reduce cell motility (Danese *et al.*, 2000; Ulett *et al.*, 2006). To investigate whether any of the identified proteins could be responsible for the MG1655Δ*cysH* phenotypes, we inactivated the corresponding genes in both MG1655 and MG1655Δ*cysH*. Although none of the three mutations resulted in a straightforward reversion to the WT phenotypes, they all resulted in a partial loss of either Congo red or calcofluor binding (or both) in the *cysH* mutant background (Fig. 4a). Inactivation of either the *slp* or *flu* genes also impaired cell adhesion to polystyrene, albeit exclusively in the

Table 3. List of upregulated proteins at 30 and 37 °C in the outer membrane-protein-enriched fraction of MG1655Δ*cysH*

GenBank accession no.	Protein name	Notes	Score*				DAve† (MG1655Δ*cysH*/MG1655)	
			MG1655		MG1655Δ*cysH*		30 °C	37 °C
			30 °C	37 °C	30 °C	37 °C		
Curli-encoding proteins								
NP_415560	CsgA	Major curlin subunit	85.34	10.29	115.35	95.37	40	160
NP_415555	CsgG	Curli production assembly/transport component	50.28	30.22	65.29	50.29	54	133
NP_415556	CsgF	Curli production assembly/transport component	65.24	10.2	120.3	35.26	60	139
Other outer membrane proteins								
NP_417963	Slp	Starvation lipoprotein	35.24	55.25	55.24	125.25	44	77
NP_415335	OmpX	Outer membrane protein X	70.26	80.26	105.29	95.26	40	35
YP_026164	Flu	Autotransporter Antigen 43	0.00	0.00	20.32	20.32	200	200

Score and DAve are both algorithms of the MAProMa software (Mauri & Dehò, 2008).

*Score is a function of the number of uniquely identified peptides in each sample.

†DAve provides a relative expression ratio between the two samples. Values of >0.1 or <-0.1 indicate differential relative expression level between two samples; a DAve value of either 200 or −200 indicates the exclusive presence of a protein in one sample.

MG1655Δ*cysH* background (Fig. 4b). Thus, our results strongly suggest that, in addition to being produced at higher levels in MG1655Δ*cysH*, the OmpX, Flu and Slp proteins contribute to its cell surface properties, such as Congo red and calcofluor binding and surface adhesion.

Inactivation of the *cysH* gene activates transcription of the *csgBAC* operon

We investigated whether increased curli production observed in the MG1655Δ*cysH* strain could be mediated by gene expression regulation of curli-encoding genes. The *csgDEFG* operon, which codes for proteins that take part in curli assembly and secretion, and for the transcription regulator CsgD, is the hub of a complex regulatory network (Römling *et al.*, 2000; Gerstel & Römling, 2003; Gerstel *et al.*, 2004; Mika & Hengge, 2013). The CsgD protein, in turn, activates the *csgBAC* operon, encoding curli subunits. Using qRT-PCR, we determined the transcript levels of *csgD* and *csgB*, representative of the two curli-encoding operons. *cysH* inactivation resulted in only a slight increase in *csgD* expression (~1.7-fold induction; data not shown). In contrast, *csgB* transcription was strongly stimulated in the MG1655Δ*cysH* mutant at both 30 and 37 °C (29- and 23-fold, respectively; Fig. 5a), in agreement with higher levels of CsgA protein (encoded by the second gene of the *csgBAC* operon) in the outer membrane fraction at both temperatures. *csgBAC* upregulation in the *cysH* mutant strain did not bypass the requirement for CsgD; indeed, *csgB* activation was almost completely lost in a MG1655Δ*cysH*Δ*csgD* double mutant (Fig. 5a). In contrast to *csgB*, expression levels for *flu*, *ompX* and *slp* genes were not altered in MG1655Δ*cysH* (data not shown), suggesting that the higher amounts of their gene products in the outer membrane preparations of this strain (Table 3) did not depend on transcription regulation of their corresponding genes.

To further confirm the role of the CysH protein in curli gene expression, we measured transcript levels of the *csgB* and *csgD* genes in the MG1655 strain overexpressing the *cysH* gene from the pT7$cysH_{wt}$ plasmid (Fig. 5b). Consistent with the results observed in the MG1655Δ*cysH* mutant, *cysH* overexpression caused a significant downregulation (fivefold) of the *csgB* gene, whilst only having a slight effect on *csgD* transcript levels (1.5-fold, Fig. 5b).

As qRT-PCR experiments strongly suggested that upregulation of *csgB* transcription in MG1655Δ*cysH* still required CsgD (Fig. 5a), we investigated whether the Congo red and calcofluor phenotype of the MG1655Δ*cysH* mutant could also be dependent on this regulator. In addition, we considered a possible role for the alternative sigma factor σ^S, which, in addition to being necessary for *csgD* transcription (Römling *et al.*, 1998b), also controls expression of the *slp* gene (Shimada *et al.*, 2004) and of several genes responsible for biosynthesis of c-di-GMP (Sommerfeldt *et al.*, 2009) – a signal molecule playing a pivotal role in regulation of cell-surface-associated structures (Tamayo *et al.*, 2007). Finally, we tested the possibility that Cbl, the regulator of

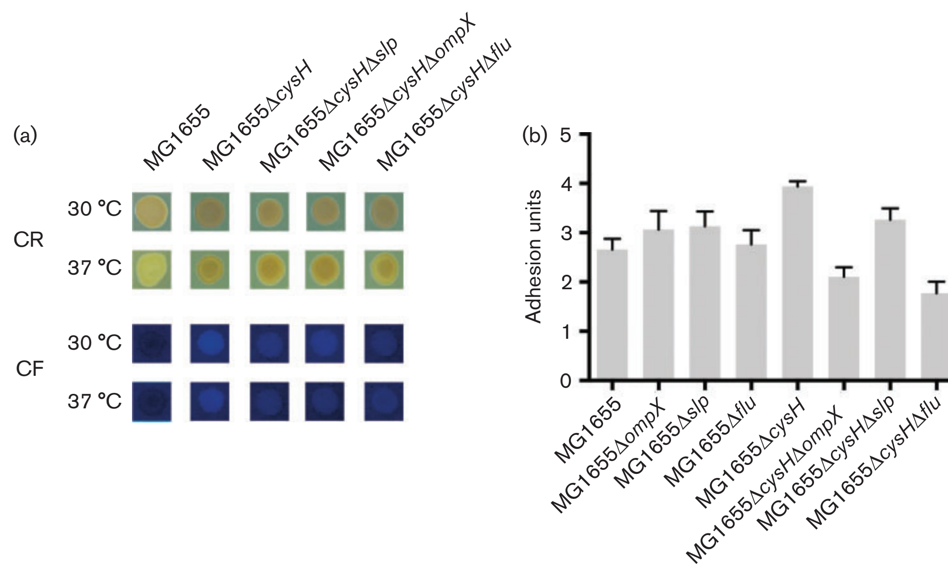

Fig. 4. (a) Effects of *slp*, *ompX* and *flu* gene inactivation in the MG1655Δ*cysH* strain on Congo red (CR) and calcofluor (CF) binding at 30 and 37 °C. Strains were grown at either 30 (for 24 h) or at 37 °C (for 18 h). Plates were incubated for 48 h at 4 °C to enhance Congo red and calcofluor binding. (b) Surface adhesion of *slp*, *ompX* and *flu* mutants to polystyrene microtitre plates. The adhesion unit values, assessed as described previously (Dorel *et al.*, 1999), are the mean ± SE of at least four independent experiments.

the organosulfonate utilization pathway, whose activity is mediated by APS, could also be the receptor protein for PAPS. In order to investigate the possible roles of CsgD, RpoS and Cbl, we inactivated the genes encoding for these regulators in the MG1655Δ*cysH* background (Fig. 5c); consistent with their involvement in the regulation of factors responsible for the MG1655Δ*cysH* phenotypes, inactivation of either *csgD* or *rpoS* affected to different extents, but did not completely abolish, Congo red and calcofluor binding. In contrast, inactivation of the *cbl* gene did not affect the Congo red and calcofluor phenotypes in either the MG1655Δ*cysH* strain (Fig. 5c) or in MG1655 (data not shown), suggesting that the Cbl protein did not mediate PAPS-dependent signalling.

DISCUSSION

The ability to sense and utilize sulfur sources appears to be tightly connected to surface adhesion and biofilm formation in *E. coli*. Indeed, mutations affecting *cysB*, encoding the master regulator of the sulfate assimilation pathway, and the *cysE* gene, whose product synthesizes *O*-acetylserine, i.e. the inducer of CysB activity, have been shown to trigger biofilm formation (Sturgill *et al.*, 2004; Ren *et al.*, 2005). Likewise, inactivation of genes involved in sulfate assimilation stimulated biofilm formation in rich medium (glucose-supplemented LB; Domka *et al.*, 2007). In addition, CysB has also been reported to control production of the siderophore pyoverdin – an important virulence factor in *Pseudomonas aeruginosa* (Imperi *et al.*, 2010). However, mutations affecting the *cysB* regulatory gene, or the sulfate assimilation pathway as a whole, likely result in general perturbation of cell physiology; indeed, *cysB* can impact carbon fluxes and modulate cAMP production (Quan *et al.*, 2002) – processes known to strongly impact biofilm formation in *E. coli* (Romeo *et al.*, 1993; Jackson *et al.*, 2002).

In this work, we have shown that inactivation of the *cysH* gene, but of no other genes in the sulfate assimilation pathway, results in enhanced cell aggregation and surface adhesion in *E. coli*. Deletion of the *cysH* gene affects outer-membrane protein composition, promoting the production of Slp, OmpX and Flu proteins, and of curli fibres (Figs 2–4, Table 3). The increase in curli fibre production involves transcription activation of the *csgBAC* operon (Fig. 5). We propose that *cysH* inactivation alters outer-membrane protein patterns and cell-surface-associated structures due to accumulation of PAPS – the substrate of the CysH (PAPS reductase) protein (Fig. 1). This modified nucleotide could act as a signal molecule by relaying to the bacterial cell, through the activity of the sulfate assimilation pathway, the availability of different sulfur sources. In this respect, PAPS would complement APS, the other modified nucleotide present as an intermediate in the sulfate assimilation pathway (Fig. 1): APS binds the regulatory protein Cbl, preventing transcription activation of genes involved in uptake and metabolism of organosulfonates, and thus allowing preferential utilization of sulfate as a sulfur source (Bykowski *et al.*, 2002). Thus, both modified nucleotides found as intermediates in the

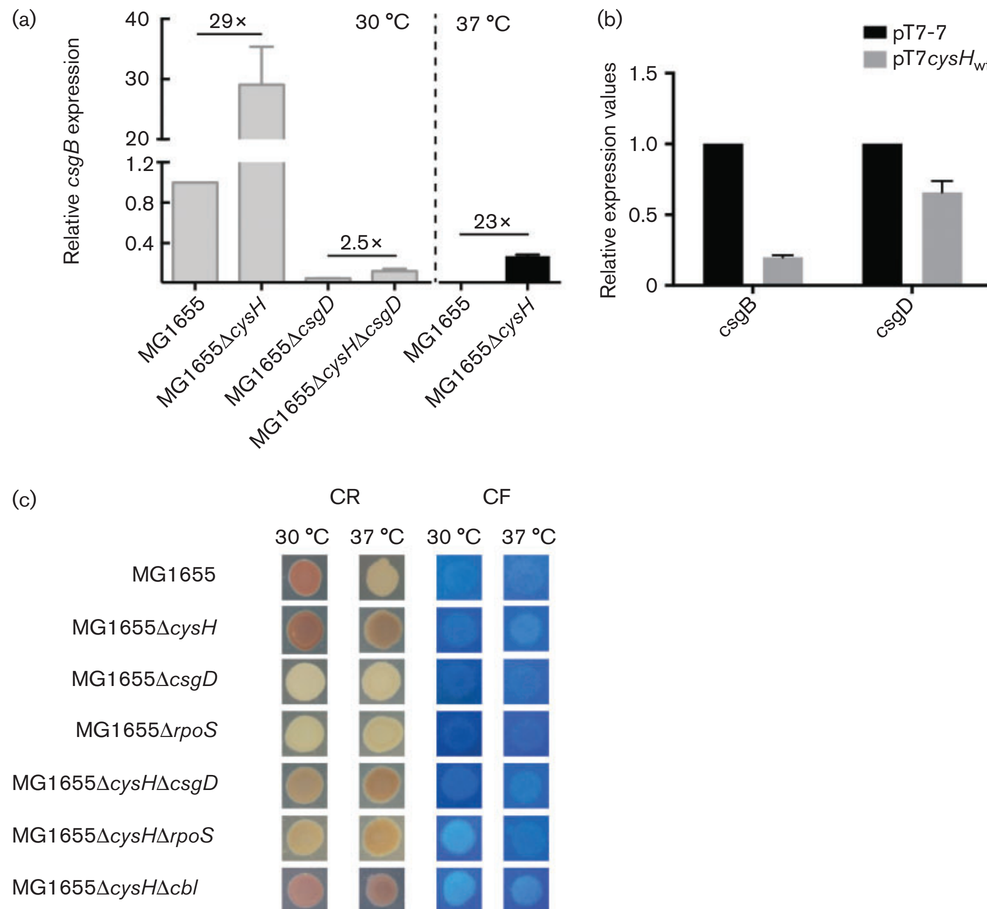

Fig. 5. (a) Relative expression levels of the *csgB* gene in strains MG1655, MG1655Δ*cysH*, MG1655Δ*csgD* and MG1655Δ*cysH*Δ*csgD* measured through qRT-PCR on overnight cultures (~18 h) grown at 30 (grey bars) and 37 °C (black bars). The *csgB* expression value in MG1655 was set to 1. Data are the mean ± SE of at least three independent experiments. (b) Effects of *cysH* overexpression on *csgB* and *csgD* transcripts in the MG1655 WT strain. The MG1655 strain was transformed with the pT7-7 vector, either empty (pT7-7) or carrying the WT allele of the *cysH* gene (pT7*cysH*$_{wt}$). The *csgB* and *csgD* expression values in MG1655 transformed with pT7-7 were set to 1. The reported values are the mean ± SD of at least two experiments performed on three RNA samples extracted from independent cultures. (c) Effects of inactivation of regulatory genes *csgD*, *rpoS* and *cbl* on Congo red (CR) and calcofluor (CF) binding. Strains were grown at either 30 (for 24 h) or 37 °C (for 18 h). Plates were incubated for 48 h at 4 °C to enhance Congo red and calcofluor binding.

sulfate assimilation pathway would act as signal molecules, although targeting different processes; whilst APS controls the utilization of sulfur sources, PAPS might have a broader activity, such as the remodulation of outer membrane proteins and extracellular structures in response to sulfur source availability.

Genetic evidence would suggest that neither CysB nor Cbl, i.e. the two regulatory proteins directly related to sulfur assimilation, are the direct target for PAPS (Figs 2a and 5c, and data not shown); thus, the molecular mechanisms of PAPS-dependent regulation remain to be identified. However, it can be speculated that PAPS accumulation in the MG1655Δ*cysH* mutant might favour translation efficiency of the *csgDEFG* mRNA, which would be consistent with the higher amounts of the CsgF and CsgG detected in the outer membrane fraction of MG1655Δ*cysH* (Table 3), and with activation of *csgB* transcription (Fig. 5a) due to increased production of its regulator, the CsgD protein. Several modified nucleotides are involved in post-transcriptional regulation, often as cofactors of enzymes involved in RNA processing and turnover, e.g. c-di-GMP and ppGpp modulate RNase activity by polynucleotide phosphorylase in *E. coli* and in actinomycetes, respectively (Siculella *et al.*, 2010; Tuckerman *et al.*, 2011). Interestingly, *E. coli* oligoribonuclease (Orn), involved in degradation of short RNA fragments, is inhibited by a PAP, i.e. the product of CysH PAPS reductase activity (Mechold *et al.*, 2006). However, depletion of PAP does not seem to be responsible for the phenotypes observed in MG1655Δ*cysH*, as mutants blocked at the upstream steps of the sulfate assimilation

pathway also do not produce PAP. In addition, the *cysQ* mutant, unable to convert PAP to AMP and phosphate, shows a weak fluorescent phenotype on calcofluor medium (Fig. 2a), probably due to inhibition of PAPS reductase activity of the CysH protein by PAP (Berendt *et al.*, 1995), leading to PAPS accumulation. A regulatory role for PAPS in cellular processes not related to sulfur metabolism is also suggested by the observations that PAPS (and also PAP) can inhibit the enzyme nucleotide diphosphate kinase (Ndk) (Schneider *et al.*, 1998), thus affecting intracellular nucleotide pools, and that CgrA, a protein carrying a PAPS-binding domain, participates in transcription regulation of *cup* fimbrial genes in *P. aeruginosa* (McManus & Dove, 2011). Future experiments will be aimed at the characterization of direct and indirect effects of PAPS accumulation, at the identification of additional targets, and at the understanding of the molecular mechanisms involved in this process.

ACKNOWLEDGEMENTS

We would like to thank Dr Maria Pasini for microscope images and Dr Stephen Michell for helpful discussions.

REFERENCES

Alexander, D. M. & St John, A. C. (1994). Characterization of the carbon starvation-inducible and stationary phase-inducible gene *slp* encoding an outer membrane lipoprotein in *Escherichia coli*. *Mol Microbiol* **11**, 1059–1071.

Barnhart, M. M., Lynem, J. & Chapman, M. R. (2006). GlcNAc-6P levels modulate the expression of curli fibers by *Escherichia coli*. *J Bacteriol* **188**, 5212–5219.

Berendt, U., Haverkamp, T., Prior, A. & Schwenn, J. D. (1995). Reaction mechanism of thioredoxin: 3′-phospho-adenylylsulfate reductase investigated by site-directed mutagenesis. *Eur J Biochem* **233**, 347–356.

Blattner, F. R., Plunkett, G., III, Bloch, C. A., Perna, N. T., Burland, V., Riley, M., Collado-Vides, J., Glasner, J. D., Rode, C. K. & other authors (1997). The complete genome sequence of *Escherichia coli* K-12. *Science* **277**, 1453–1462.

Bougdour, A., Lelong, C. & Geiselmann, J. (2004). Crl, a low temperature-induced protein in *Escherichia coli* that binds directly to the stationary phase sigma subunit of RNA polymerase. *J Biol Chem* **279**, 19540–19550.

Brombacher, E., Baratto, A., Dorel, C. & Landini, P. (2006). Gene expression regulation by the curli activator CsgD protein: modulation of cellulose biosynthesis and control of negative determinants for microbial adhesion. *J Bacteriol* **188**, 2027–2037.

Brown, P. K., Dozois, C. M., Nickerson, C. A., Zuppardo, A., Terlonge, J. & Curtiss, R., III (2001). MlrA, a novel regulator of curli (AgF) and extracellular matrix synthesis by *Escherichia coli* and *Salmonella enterica* serovar Typhimurium. *Mol Microbiol* **41**, 349–363.

Bykowski, T., van der Ploeg, J. R., Iwanicka-Nowicka, R. & Hryniewicz, M. M. (2002). The switch from inorganic to organic sulphur assimilation in *Escherichia coli*: adenosine 5′-phosphosulphate (APS) as a signalling molecule for sulphate excess. *Mol Microbiol* **43**, 1347–1358.

Carzaniga, T., Antoniani, D., Dehò, G., Briani, F. & Landini, P. (2012). The RNA processing enzyme polynucleotide phosphorylase negatively controls biofilm formation by repressing poly-*N*-acetylglucosamine (PNAG) production in *Escherichia coli* C. *BMC Microbiol* **12**, 270.

Comunian, C., Rusconi, F., De Palma, A., Brunetti, P., Catalucci, D. & Mauri, P. L. (2011). A comparative MudPIT analysis identifies different expression profiles in heart compartments. *Proteomics* **11**, 2320–2328.

Cookson, A. L., Cooley, W. A. & Woodward, M. J. (2002). The role of type 1 and curli fimbriae of Shiga toxin-producing *Escherichia coli* in adherence to abiotic surfaces. *Int J Med Microbiol* **292**, 195–205.

Danese, P. N., Pratt, L. A., Dove, S. L. & Kolter, R. (2000). The outer membrane protein, antigen 43, mediates cell-to-cell interactions within *Escherichia coli* biofilms. *Mol Microbiol* **37**, 424–432.

Datsenko, K. A. & Wanner, B. L. (2000). One-step inactivation of chromosomal genes in *Escherichia coli* K-12 using PCR products. *Proc Natl Acad Sci U S A* **97**, 6640–6645.

Domka, J., Lee, J., Bansal, T. & Wood, T. K. (2007). Temporal gene-expression in *Escherichia coli* K-12 biofilms. *Environ Microbiol* **9**, 332–346.

Dorel, C., Vidal, O., Prigent-Combaret, C., Vallet, I. & Lejeune, P. (1999). Involvement of the Cpx signal transduction pathway of *E. coli* in biofilm formation. *FEMS Microbiol Lett* **178**, 169–175.

DuBois, M., Gilles, K. A., Hamilton, J. K., Rebers, P. A. & Smith, F. (1956). Colorimetric method for determination of sugars and related substances. *Anal Chem* **28**, 350–356.

Garavaglia, M., Rossi, E. & Landini, P. (2012). The pyrimidine nucleotide biosynthetic pathway modulates production of biofilm determinants in *Escherichia coli*. *PLoS ONE* **7**, e31252.

Gerstel, U. & Römling, U. (2001). Oxygen tension and nutrient starvation are major signals that regulate *agfD* promoter activity and expression of the multicellular morphotype in *Salmonella typhimurium*. *Environ Microbiol* **3**, 638–648.

Gerstel, U. & Römling, U. (2003). The *csgD* promoter, a control unit for biofilm formation in *Salmonella typhimurium*. *Res Microbiol* **154**, 659–667.

Gerstel, U., Park, C. & Römling, U. (2003). Complex regulation of *csgD* promoter activity by global regulatory proteins. *Mol Microbiol* **49**, 639–654.

Gualdi, L., Tagliabue, L. & Landini, P. (2007). Biofilm formation-gene expression relay system in *Escherichia coli*: modulation of sigmaS-dependent gene expression by the CsgD regulatory protein via sigmaS protein stabilization. *J Bacteriol* **189**, 8034–8043.

Hammar, M., Arnqvist, A., Bian, Z., Olsén, A. & Normark, S. (1995). Expression of two *csg* operons is required for production of fibronectin- and Congo red-binding curli polymers in *Escherichia coli* K-12. *Mol Microbiol* **18**, 661–670.

Harrington, B. J. & Raper, K. B. (1968). Use of a fluorescent brightener to demonstrate cellulose in the cellular slime molds. *Appl Microbiol* **16**, 106–113.

Hung, D. L., Raivio, T. L., Jones, C. H., Silhavy, T. J. & Hultgren, S. J. (2001). Cpx signaling pathway monitors biogenesis and affects assembly and expression of P pili. *EMBO J* **20**, 1508–1518.

Imperi, F., Tiburzi, F., Fimia, G. M. & Visca, P. (2010). Transcriptional control of the *pvdS* iron starvation sigma factor gene by the master regulator of sulfur metabolism CysB in *Pseudomonas aeruginosa*. *Environ Microbiol* **12**, 1630–1642.

Jackson, D. W., Simecka, J. W. & Romeo, T. (2002). Catabolite repression of *Escherichia coli* biofilm formation. *J Bacteriol* **184**, 3406–3410.

Kader, A., Simm, R., Gerstel, U., Morr, M. & Römling, U. (2006). Hierarchical involvement of various GGDEF domain proteins in rdar morphotype development of *Salmonella enterica* serovar Typhimurium. *Mol Microbiol* **60**, 602–616.

Kredich, N. M. (1992). The molecular basis for positive regulation of *cys* promoters in *Salmonella typhimurium* and *Escherichia coli*. *Mol Microbiol* **6**, 2747–2753.

Liu, C., Martin, E. & Leyh, T. S. (1994). GTPase activation of ATP sulfurylase: the mechanism. *Biochemistry* **33**, 2042–2047.

Mauri, P. & Dehò, G. (2008). A proteomic approach to the analysis of RNA degradosome composition in *Escherichia coli*. *Methods Enzymol* **447**, 99–117.

Mauri, P., Scarpa, A., Nascimbeni, A. C., Benazzi, L., Parmagnani, E., Mafficini, A., Della Peruta, M., Bassi, C., Miyazaki, K. & Sorio, C. (2005). Identification of proteins released by pancreatic cancer cells by multidimensional protein identification technology: a strategy for identification of novel cancer markers. *FASEB J* **19**, 1125–1127.

McManus, H. R. & Dove, S. L. (2011). The CgrA and CgrC proteins form a complex that positively regulates *cupA* fimbrial gene expression in *Pseudomonas aeruginosa*. *J Bacteriol* **193**, 6152–6161.

Mechold, U., Ogryzko, V., Ngo, S. & Danchin, A. (2006). Oligoribonuclease is a common downstream target of lithium-induced pAp accumulation in *Escherichia coli* and human cells. *Nucleic Acids Res* **34**, 2364–2373.

Mecsas, J., Welch, R., Erickson, J. W. & Gross, C. A. (1995). Identification and characterization of an outer membrane protein, OmpX, in *Escherichia coli* that is homologous to a family of outer membrane proteins including Ail of *Yersinia enterocolitica*. *J Bacteriol* **177**, 799–804.

Mika, F. & Hengge, R. (2013). Small regulatory RNAs in the control of motility and biofilm formation in *E. coli* and *Salmonella*. *Int J Mol Sci* **14**, 4560–4579.

Mikkelsen, H., Sivaneson, M. & Filloux, A. (2011). Key two-component regulatory systems that control biofilm formation in *Pseudomonas aeruginosa*. *Environ Microbiol* **13**, 1666–1681.

Neidhardt, F. C., Bloch, P. L. & Smith, D. F. (1974). Culture medium for enterobacteria. *J Bacteriol* **119**, 736–747.

Otto, K. & Hermansson, M. (2004). Inactivation of *ompX* causes increased interactions of type 1 fimbriated *Escherichia coli* with abiotic surfaces. *J Bacteriol* **186**, 226–234.

Palma, C.-A., Samorì, P. & Cecchini, M. (2010). Atomistic simulations of 2D bicomponent self-assembly: from molecular recognition to self-healing. *J Am Chem Soc* **132**, 17880–17885.

Plumbridge, J. A. (1991). Repression and induction of the nag regulon of *Escherichia coli* K-12: the roles of *nagC* and *nagA* in maintenance of the uninduced state. *Mol Microbiol* **5**, 2053–2062.

Pratt, L. A. & Silhavy, T. J. (1998). Crl stimulates RpoS activity during stationary phase. *Mol Microbiol* **29**, 1225–1236.

Prigent-Combaret, C., Prensier, G., Le Thi, T. T., Vidal, O., Lejeune, P. & Dorel, C. (2000). Developmental pathway for biofilm formation in curli-producing *Escherichia coli* strains: role of flagella, curli and colanic acid. *Environ Microbiol* **2**, 450–464.

Prigent-Combaret, C., Brombacher, E., Vidal, O., Ambert, A., Lejeune, P., Landini, P. & Dorel, C. (2001). Complex regulatory network controls initial adhesion and biofilm formation in *Escherichia coli* via regulation of the *csgD* gene. *J Bacteriol* **183**, 7213–7223.

Quan, J. A., Schneider, B. L., Paulsen, I. T., Yamada, M., Kredich, N. M. & Saier, M. H., Jr (2002). Regulation of carbon utilization by sulfur availability in *Escherichia coli* and *Salmonella typhimurium*. *Microbiology* **148**, 123–131.

R Development Core Team (2013). *R: A Language and Environment for Statistical Computing*. Vienna: R Foundation for Stistical Computing.

Ren, D., Zuo, R., González Barrios, A. F., Bedzyk, L. A., Eldridge, G. R., Pasmore, M. E. & Wood, T. K. (2005). Differential gene expression for investigation of *Escherichia coli* biofilm inhibition by plant extract ursolic acid. *Appl Environ Microbiol* **71**, 4022–4034.

Romeo, T. (1998). Global regulation by the small RNA-binding protein CsrA and the non-coding RNA molecule CsrB. *Mol Microbiol* **29**, 1321–1330.

Romeo, T., Gong, M., Liu, M. Y. & Brun-Zinkernagel, A. M. (1993). Identification and molecular characterization of *csrA*, a pleiotropic gene from *Escherichia coli* that affects glycogen biosynthesis, gluconeogenesis, cell size, and surface properties. *J Bacteriol* **175**, 4744–4755.

Römling, U., Sierralta, W. D., Eriksson, K. & Normark, S. (1998a). Multicellular and aggregative behaviour of *Salmonella typhimurium* strains is controlled by mutations in the *agfD* promoter. *Mol Microbiol* **28**, 249–264.

Römling, U., Bian, Z., Hammar, M., Sierralta, W. D. & Normark, S. (1998b). Curli fibers are highly conserved between *Salmonella typhimurium* and *Escherichia coli* with respect to operon structure and regulation. *J Bacteriol* **180**, 722–731.

Römling, U., Rohde, M., Olsén, A., Normark, S. & Reinköster, J. (2000). AgfD, the checkpoint of multicellular and aggregative behaviour in *Salmonella typhimurium* regulates at least two independent pathways. *Mol Microbiol* **36**, 10–23.

Schneider, B., Xu, Y. W., Janin, J., Véron, M. & Deville-Bonne, D. (1998). 3′-Phosphorylated nucleotides are tight binding inhibitors of nucleoside diphosphate kinase activity. *J Biol Chem* **273**, 28773–28778.

Shimada, T., Makinoshima, H., Ogawa, Y., Miki, T., Maeda, M. & Ishihama, A. (2004). Classification and strength measurement of stationary-phase promoters by use of a newly developed promoter cloning vector. *J Bacteriol* **186**, 7112–7122.

Siculella, L., Damiano, F., di Summa, R., Tredici, S. M., Alduina, R., Gnoni, G. V. & Alifano, P. (2010). Guanosine 5′-diphosphate 3′-diphosphate (ppGpp) as a negative modulator of polynucleotide phosphorylase activity in a 'rare' actinomycete. *Mol Microbiol* **77**, 716–729.

Sohanpal, B. K., El-Labany, S., Lahooti, M., Plumbridge, J. A. & Blomfield, I. C. (2004). Integrated regulatory responses of *fimB* to *N*-acetylneuraminic (sialic) acid and GlcNAc in *Escherichia coli* K-12. *Proc Natl Acad Sci U S A* **101**, 16322–16327.

Sommerfeldt, N., Possling, A., Becker, G., Pesavento, C., Tschowri, N. & Hengge, R. (2009). Gene expression patterns and differential input into curli fimbriae regulation of all GGDEF/EAL domain proteins in *Escherichia coli*. *Microbiology* **155**, 1318–1331.

Soo, V. W. C. & Wood, T. K. (2013). Antitoxin MqsA represses curli formation through the master biofilm regulator CsgD. *Sci Rep* **3**, 3186.

Sturgill, G., Toutain, C. M., Komperda, J., O'Toole, G. A. & Rather, P. N. (2004). Role of CysE in production of an extracellular signaling molecule in *Providencia stuartii* and *Escherichia coli*: loss of CysE enhances biofilm formation in *Escherichia coli*. *J Bacteriol* **186**, 7610–7617.

Tagliabue, L., Maciag, A., Antoniani, D. & Landini, P. (2010a). The *yddV-dos* operon controls biofilm formation through the regulation of genes encoding curli fibers' subunits in aerobically growing *Escherichia coli*. *FEMS Immunol Med Microbiol* **59**, 477–484.

Tagliabue, L., Antoniani, D., Maciag, A., Bocci, P., Raffaelli, N. & Landini, P. (2010b). The diguanylate cyclase YddV controls production of the exopolysaccharide poly-*N*-acetylglucosamine (PNAG) through regulation of the PNAG biosynthetic *pgaABCD* operon. *Microbiology* **156**, 2901–2911.

Tamayo, R., Pratt, J. T. & Camilli, A. (2007). Roles of cyclic diguanylate in the regulation of bacterial pathogenesis. *Annu Rev Microbiol* **61**, 131–148.

Teather, R. M. & Wood, P. J. (1982). Use of Congo red–polysaccharide interactions in enumeration and characterization of cellulolytic bacteria from the bovine rumen. *Appl Environ Microbiol* **43**, 777–780.

Toledano, M. B., Kumar, C., Le Moan, N., Spector, D. & Tacnet, F. (2007). The system biology of thiol redox system in *Escherichia coli* and yeast: differential functions in oxidative stress, iron metabolism and DNA synthesis. *FEBS Lett* **581**, 3598–3607.

Tuckerman, J. R., Gonzalez, G. & Gilles-Gonzalez, M.-A. (2011). Cyclic di-GMP activation of polynucleotide phosphorylase signal-dependent RNA processing. *J Mol Biol* **407**, 633–639.

Uhlich, G. A., Chen, C.-Y., Cottrell, B. J. & Nguyen, L.-H. (2014). Growth media and temperature effects on biofilm formation by serotype O157 : H7 and non-O157 Shiga toxin-producing *Escherichia coli*. *FEMS Microbiol Lett* **354**, 133–141.

Ulett, G. C., Webb, R. I. & Schembri, M. A. (2006). Antigen-43-mediated autoaggregation impairs motility in *Escherichia coli*. *Microbiology* **152**, 2101–2110.

van der Ploeg, J. R., Eichhorn, E. & Leisinger, T. (2001). Sulfonate-sulfur metabolism and its regulation in *Escherichia coli*. *Arch Microbiol* **176**, 1–8.

Vidal, O., Longin, R., Prigent-Combaret, C., Dorel, C., Hooreman, M. & Lejeune, P. (1998). Isolation of an *Escherichia coli* K-12 mutant strain able to form biofilms on inert surfaces: involvement of a new *ompR* allele that increases curli expression. *J Bacteriol* **180**, 2442–2449.

Vogt, J. & Schulz, G. E. (1999). The structure of the outer membrane protein OmpX from *Escherichia coli* reveals possible mechanisms of virulence. *Structure* **7**, 1301–1309.

Weber, H., Pesavento, C., Possling, A., Tischendorf, G. & Hengge, R. (2006). Cyclic-di-GMP-mediated signalling within the sigma network of *Escherichia coli*. *Mol Microbiol* **62**, 1014–1034.

Zheng, D., Constantinidou, C., Hobman, J. L. & Minchin, S. D. (2004). Identification of the CRP regulon using *in vitro* and *in vivo* transcriptional profiling. *Nucleic Acids Res* **32**, 5874–5893.

Edited by: D. Grainger